DIGITAL VERSUS ANALOG GRADED-GAP QUANTUM WELLS IN THE PRESENCE OF APPLIED CONSTANT ELECTRIC FIELD

Ass. Prof. M.Sc. Miteva A. M.
Space Research and Technology Institute – Bulgarian Academy of Sciences, Sofia, Bulgaria

ad.miteva@gmail.com

Abstract: *In this paper we study in detail the influence of the longitudinal constant electric field on the energy values of a digital quantum well $Al_xGa_{1-x}As/GaAs$ structure and its equivalent graded-composition analog quantum well. We calculate the energies of the electron and hole bound states, the energies of the main optical transitions and their Stark shifts. The spatial distributions of the main electronic and hole states at various given values of the applied electric field are also calculated. The semi-empirical tight-binding approximation in the spin dependent sp^3s^* basis is used and is carried out by surface Green function matching employing an algorithm previously developed and used to study inhomogeneous systems. The aim of these calculations is to find out in detail to what extent these two structures have similar or different properties in the presence of an applied electric field. We compare our results with the results for the conventional rectangular quantum well and with the available experimental data for quantum wells with similar parameters.*

Keywords: DIGITAL AND ANALOG GROWTH TECHNIQUES, QUANTUM CONFINED STARK EFFECT, GRADED-GAP QUANTUM WELLS, AlGaAs, TIGHT-BINDING METHOD, ELECTRONIC STATES IN QUANTUM WELLS

1. Introduction

Nowadays, semiconductor nanostructures (superlattices and quantum wells) are already employed in electronic and optoelectronic devices. This possibility is due to the ability of modern crystal growers to make good quality composition semiconductor heterostructures with very small dimensions. Many semiconductor devices with built-in quantum wells work under application of an electric field [1].

In semiconductor quantum wells (QWs), sharp excitonic absorption peaks are clearly observed even at room temperature. When an electric field is applied perpendicular to the QW layers, the energy of the fundamental absorption edge shifts by a large amount without severe broadening of the exciton resonance. This is the well-known quantum confined Stark effect (QCSE). These properties enable one to utilize QWs for high-performance room temperature optoelectronic devices. Moreover, to improve the performance of these optical devices, band structure modifications in QWs have also been investigated. The electric field effects (Stark effects) on the graded-gap QW structures, where the band gap of the well is inclined along the growth direction, are one of the most promising among the modifications for applications of making various fast optoelectronic devices [1-4]. The modification of the well potential shape can create different optical properties and thus optimize nanostructure-based devices compared to conventional rectangular QWs (RQWs).

In this paper we present a realistic tight-binding (TB) numerical calculation of the energy values for the main bound electronic and hole states as well as their spatial distributions in graded-gap QWs of two different types – analog (AQW) and digital (DQW) without and under application of a constant electric field *F*. AQWs are realized by the analog alloy method by varying the alloy composition linearly in the AlGaAs well layer, i.e. one growth directly inhomogeneous QWs with different composition profiles. However, with this experimental growth method, it is technically difficult to control the alloy composition precisely in the narrow well region, and there will be some structural non-uniformities along the QW. To solve this problem, an alternative approach called the digital alloy approximation was applied in [5,6]. In this approach a supposedly equivalent QW is growing, where the AQW is being replaced by a sequence of wells and barriers with the same well depth but with a programmed sequence of varying widths. Although analog and digital structures are regarded as equivalent, some doubts have been raised [5-8].

The aim of the present work is to explore this issue further in terms of a realistic model, which allows one to calculate not only average properties but also detailed features. A comparative study will be carried out of the two structures shown in Fig. 1 as a practical example of analog versus digital QWs under an applied electric field.

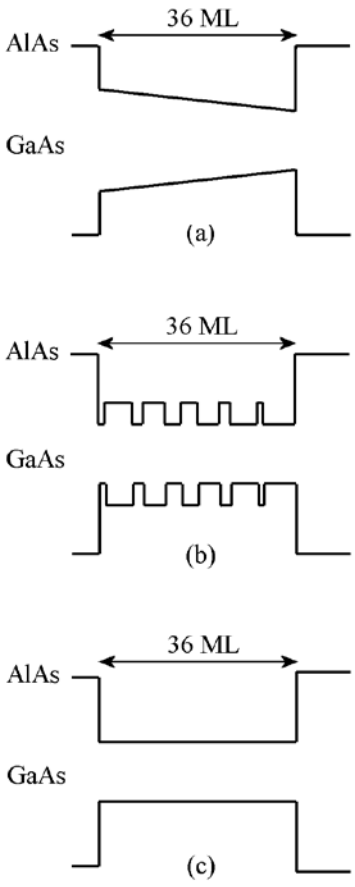

Fig. 1 *Schematic band diagram of: (a) genuine analog graded-gap QW (AQW); (b) the equivalent digital graded-gap QW (DQW); (c) conventional rectangular QW (RQW). (a) The alloy composition of $Al_xGa_{1-x}As$ in the well varies linearly from x=0.3 to x=0.0 (from the left to the right side of the QW). (b) The alloy composition x of the inserted $Al_xGa_{1-x}As$ barrier layers is 0.3, the minimum width of the structure is one monolayer (ML), the composition of the wells of the inserted region is x=0. (c) The alloy composition x of the well is 0, i.e. pure GaAs. In these three cases we have pure AlAs at the barriers.*

2. Model and Method

We study $AlAs/Al_xGa_{1-x}As/AlAs$ QWs with the graded-gap well structures (Figure 1). The external constant electric field *F* is applied to the QWs parallel to the growth axis [001]. Similar

structure is partially investigated experimentally and theoretically in [6,7]. Theoretical works about the electric field effect in analog and digital QW systems have been done mainly in the effective mass approximation. In the calculations we use the sp^3s^* spin-dependent semi-empirical tight-binding model as it is described in [8-11]. The virtual crystal approximation is used for the description of the TB parameters TB(x) for the ternary compound $Al_xGa_{1-x}As$:

(1) $TB(x) = x.TB(AlAs) + (1 - x).TB(GaAs).$

The surface Green function matching technique is developed in [9-12] and is applied for calculating the Green function of the infinite system (AlAs) containing the finite inhomogenious slab. Here the presence of an external static electric field is defined similarly to [13,14], by adding a linearly varying with the distance term Δ_n to the diagonal elements of the TB Hamiltonian matrix:

(2) $TB(n, x) = TB(x) + \Delta_n, \quad \Delta_n = (n - 1).F.(a/4),$

where a is the lattice constant, F is the intensity of the longitudinal constant electric field, TB(x) are the diagonal TB parameters without an electric field for the bulk material with Al concentration x, and n is the number of the layers (i.e. layer index) in the QW. The electric field F is applied to the structure under study at two points in the barrier regions (AlAs) situated at the distance of 5 monolayers (MLs) from the edges of the graded-gap QWs. The width of both QWs under study is 36 MLs (102 Å). The zero value of the intensity of applied electric field F is defined at the point which corresponds to 5 MLs from the left edge of the QWs. In numerical calculations we use a wide range of electric fields, from -200 to +200 kV/cm with a step of 5 kV/cm. We also made calculations for the conventional rectangular QW (RQW) in order to compare it with our results. The RQW has a 36 MLs (102 Å) GaAs well and AlAs barriers. The calculations are made at the center of the two-dimensional Brillouin zone.

3. Results and Discussion

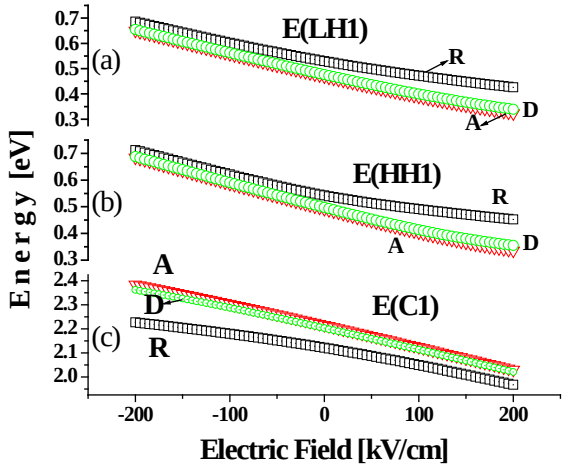

Fig. 2. *The dependence of the ground state energies for: (a) – E(LH1) light holes; (b) – E(HH1) heavy holes; (c) – E(C1) electrons, on the applied electric field strength; A (AQW) – red triangles, D (DQW) – green circles, R (RQW) – black squares.*

Figure 2 displays the calculated ground state energies of the conduction E(C1) and valence E(HH1), E(LH1) states in the three kinds of QWs studied versus the applied constant electric field. We notice that the electric field effects are similar for all QWs under consideration. For the valence states, at the same value of the electric field F, the Stark effects are stronger for the AQW and the DQW, than for the RQW. For the electron energy the tendency is opposite.

Figure 3(a) shows the dependence of the main optical transition energy E(C1-HH1) from the electric field for the three QWs. Here a similar dependence is observed: the influence of the electric field on these QWs is qualitative equal. When increasing the applied electric field, the transition energy decreases. In the whole range of the electric field, the value of the energy E(C1-HH1) for AQW is greater than for the corresponding value for the DQW. Figure 3(b) shows the dependence of the main optical transition energy E(C1-LH1) from the electric field for the three QWs. The influence of the electric field for the three QWs is similar to E(C1-HH1). The transition energy decreases with increasing of applied electric field.

Figure 4(a) shows the Stark shifts of the main optical transition energy E(C1-HH1) from the applied external constant electric field for the three QWs. The Stark shift of the energy is defined as the absolute value of the difference of this energy at a given electric field minus the value of this energy at field zero. The dependence of the Stark shift for the three QWs is similar. The increase of the field increases the Stark shifts. This increasing is better pronounced for DQW than for AQW, for all values of the field F. This increasing is also better pronounced for RQW than for both DQW and AQW, in the region of large values of the applied electric field. For low electric fields (smaller than ~ 25 kV/cm) the Stark shifts of RQW are smaller than for both DQW and AQW. The conclusion is that DQW structure probably will be applicable to high-speed optical modulators with low driving voltages. Figure 4(b) shows the same as Figure 4(a) but for the transition energy E(C1-LH1). Here one can see that the influence of the electric filed on the Stark shifts in the three QWs is similar to E(C1-HH1). The Stark shifts decrease with the increase of the applied field.

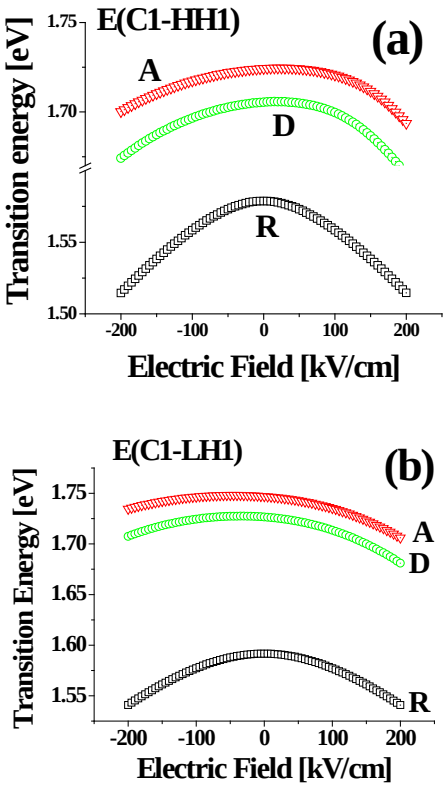

Fig. 3. *The dependence of the main transition energies: (a) E(C1-HH1) and (b) E(C1-LH1) on the applied electric field; A (AQW) –red triangles, D (DQW) – green circles, R (RQW) – black squares.*

Table 1 gives some differences of the Stark shifts measured and calculated for DQW and RQW in [6] (see Figure 3, [6]). These results are compared with the calculated here results with the tight-binding model described above. The calculation in [6] was done in the effective mass approximation. The experimental data for the Stark shifts in [6] were obtained by absorption current spectroscopy method. The discrepancies are likely due to the difference between real and ideal DQW structures. However, the calculated values are for the ideal QW, which actually differs from that of the measured composition profile. Here the Stark shift energies were calculated not at room temperature but at temperature T = 0K. That is the exciton effects are not included in the calculations.

The results of the total spectral strength spatial distributions are depicted in Figures 5, 6 and 7. The applied electric field intensity F is respectively 0 kV/cm, -50 kV/cm and -100 kV/cm. For the three QWs there is a complete overlap of the spatial distributions at F=0. A displacement of the spatial distributions of C1, HH1 and LH1 states appears at electric field $F \neq 0$. It is larger for analog and digital QWs than for rectangular QW. In the DQW case some features begin to emerge and reflect its multiwell structure [8]. This type of behavior, of course, never appears in an AQW.

Similar results concerning the calculation of the ground state energies of the conduction E(C1) and valence E(HH1), E(LH1) states in three QWs in dependance of applied constant electric field F were already published and discussed in [7].

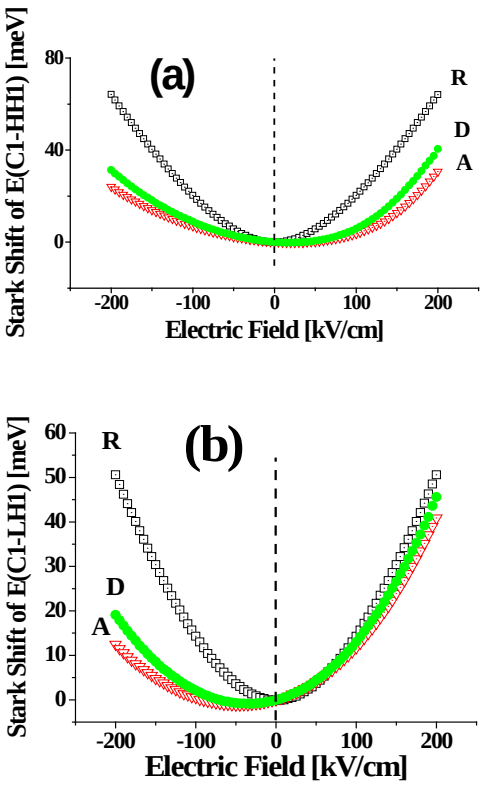

Fig.4*. The Stark shifts of the main transition energies: (a) energy shift of E(C1-HH1) and (b) the same for the energy E(C1-LH1); A (AQW) – red triangles, D (DQW) – green circles, R (RQW) – black squares.*

Table 1: *A comparison of the calculated values with the calculated and experimental values from the literature [6] for the Stark shifts (in meV) of E(C1-HH1) for AQWs, DQWs and RQWs.*

El. field F, [kV/cm]	Stark shift of E(C1-HH1), [meV]						
	RQW			DQW			AQW
	This work	[6]		This work	[6]		This work
		Theor.	Exp.		Theor.	Exp.	
50	5,7	4		2,9	7,5		2,2
100	20,3	14		8,9	18,2		6,9
20	0,8		0,38	0,8			0,6
25	1,5		0,85	1,1			0,9
35	2,9		1,3	1,7			1,4
10	0,1			0,4		0,9	0,3
60	8			3,8		9,4	3
90	16,9			7,4		13	5,8

4. Conclusion

The real purpose of this calculation is to make a detailed comparative study of the AQW and DQW structures in the presence of applied electric field. We also would like to demonstrate the practical use of the applied calculation method. Although the two QW structures are considered as equivalent, there is lack of detailed investigation on this issue. Our calculations allow a detailed electronic structure investigation of AQWs and DQWs in the presence of a constant electric field. On the basis of a realistic model calculation, we show that even in the Stark shifts of the main electronic energies there are some small differences in the AQW and DQW [7]. Nevertheless the energy eigenvalues of these two QWs are quite similar they have some different properties [7]. We find also differences in the spatial distributions of the electron and hole spectral strength for these two QWs. In the case of DQW, its multiwell nature becomes quite obvious.

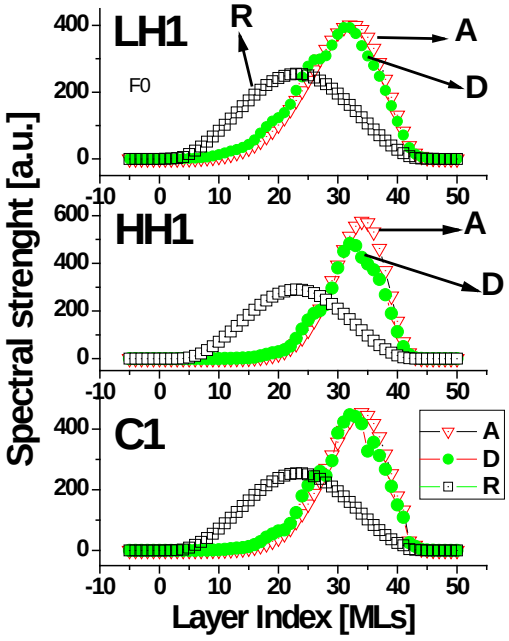

Fig. 5. *Spatial distributions of the total spectral strength for C1, HH1 and LH1 states in A (AQW) – red triangles, D (DQW) – green circles, R (RQW) – black squares. The electric field intensity is 0 kV/cm.*

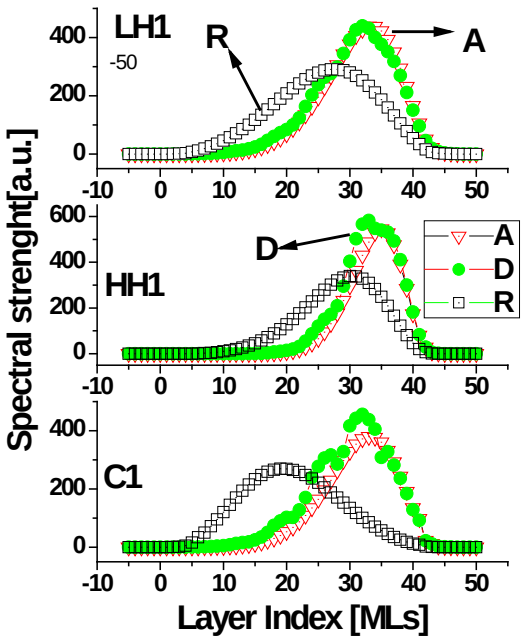

Fig. 6. *Spatial distributions of the total spectral strength for C1, HH1 and LH1 states in A (AQW) – red triangles, D (DQW) – green circles, R (RQW) – black squares. The electric field intensity is -50 kV/cm.*

The actual composition profiles experimentally obtained may differ significantly from those of the ideal DQW stricture. Then a

more realistic calculation would require taking account of the measured composition profile. With the method used here there would be no difficulty in taking in full account of any details of a realistic model that one might want to study. The work is in progress in this direction.

Such investigations will help to find a QW potential profile with better Stark effect characteristics. The investigation of the electric field effects on the optical properties of the QW structures with graded-gap potential profiles is essential for the optimization of QW-based devices.

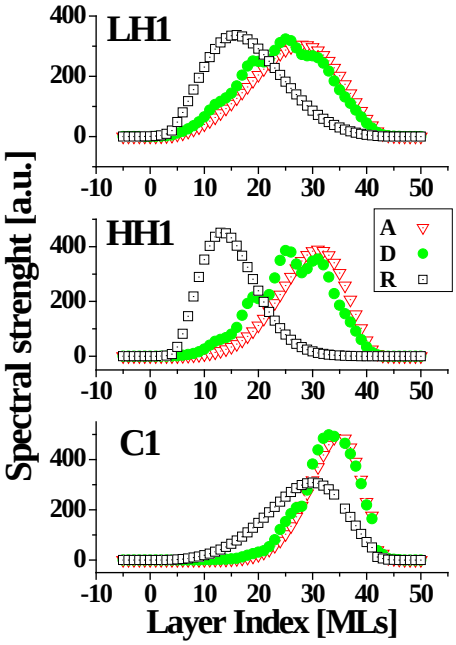

Fig. 7. *Spatial distributions of the total spectral strength for C1, HH1 and LH1 states in A (AQW) – red triangles, D (DQW) – green circles, R (RQW) – black squares. The electric field intensity is -100 kV/cm.*

5. References

1. Di Carlo A., Microscopic theory of nanostructured semiconductor devices: beyond the envelope-function approximation, Semicond. Sci. Technol., 18, 2003, R1-R31.
2. Singh J., Physics of Semiconductors and Heterostructures, Singapore, McGraw-Hill Book Co., 1993.
3. Weisbuch C., B. Vinter, Quantum Semiconductor Structures, London, Academic Press Limited, 1991.
4. Bouzekova-Penkova A., About the properties of some nanostructures with uniform electric field presence, Proceedings of 26-th International Scientific Conference, 13-16 September, 2010, Sozopol, Bulgaria, 2010, 300-305.
5. Zhao H., S. M. Wang1, Q. X. Zhao, Z. H. Lai, M. Sadeghi, A. Larsson, Comparison of optical and structural quality of GaIn(N)As analog and digital quantum wells grown by molecular beam epitaxy, Semicond. Sci. Technol., 23, 2008, 125002-125007.
6. Ishikawa T., K. Tada, Observation of Quantum-Confined Stark Effect in a Graded-Gap Quantum WellJpn. J. Appl. Phys., 28, 1989, L1982-L1984.
7. Miteva A. M., S. J. Vlaev, Electric field influence on the electronic states of digital versus analog graded-gap quantum wells, In: Nanoscience&Nanotechnology 9, eds. E. Balabanova, I. Dragieva, Sofia, Heron Press, 2009, 21-23.
8. Vlaev S. J., F. Garcia-Moliner, V. R. Velasco, Electronic states of digital versus analog graded quantum wells, Phys. Rev. B, 52, 1995, 13784-13787.
9. Vlaev S. J., V. R. Velasco, F. Garcia-Moliner, Electronic states in graded-composition heterostructures, Phys. Rev. B, 49, 1994, 11222-11229.
10. Vlaev S. J., V. R. Velasco, F. Garcia-Moliner, Tight-binding calculation of electronic states in a triangular symmetrical quantum well, Phys. Rev. B, 50, 1994, 4577 – 4580.
11. Vlaev S. J., V. R. Velasco, F. Garcia-Moliner, Tight-binding calculation of electronic states in an inverse parabolic quantum well, Phys. Rev. B, 51, 1995, 7321 - 7324.
12. Garcia-Moliner F., V. R. Velasco, Theory of Single and Multiple Interfaces. The Method of Surface Green Function Matching, Singapore, World Scientific, 1993.
13. Vlaev S. J., A. M. Miteva, D. A. Contreras-Solorio, V. R. Velasco, Stark shift effects in rectangular and graded gap quantum wells, Surf. Sci., 424, 1999, 331-339.
14. Vlaev S. J., A. M. Miteva, D. A. Contreras-Solorio, V. R. Velasco, Stark effect in diffused quantum wells, Superlat. and Microstruct., 26, 1999, 325-332.